PAPER • OPEN ACCESS

Assessment of the corrosion susceptibility of 434 ferritic stainless steel in chloride-sulphate solution

To cite this article: Roland T. Loto 2021 *IOP Conf. Ser.: Mater. Sci. Eng.* **1186** 012005

View the article online for updates and enhancements.

Assessment of the corrosion susceptibility of 434 ferritic stainless steel in chloride-sulphate solution

Roland T. Loto[1]

[1]Department of Mechanical Engineering, Covenant University, Ogun state, Nigeria

Email: tolulope.loto@covenantuniversity.edu.ng

Abstract. The corrosion polarization behaviour of 434 ferritic stainless (434ST) was studied in 1 M H_2SO_4 at 0.25% to 2% NaCl concentration through potentiodynamic polarization techniques and open circuit potential analysis. Results showed corrosion rate of 434ST at in 1 M H_2SO_4 solution at 0% NaCl concentration is 5.51 mm/y. However, at 0.25% NaCl concentration corrosion output decreased to 1.31 mm/y due to competitive adsorption mechanism with dissolved O_2 atoms. Increment in NaCl concentration causes increase in corrosion rate till 1% NaCl concentration at 5.97 mm/y. After 1% NaCl concentration, the corrosion of 434ST attained threshold deterioration mechanism with values varying between 6.20 mm/y and 6.56 mm/y. Shift in corrosion potential plot with respect to 434ST at 0% NaCl concentration indicates anodic corrosion and passivation mechanism on the steel surface which was also proven from the anodic Tafel slope values. Open circuit potential plots showed plots at 2% NaCl concentration showed the least thermodynamic tendency to corrode with the strongest shift to electropositive potentials which culminated at -0.439 V at 5400 s of observation. The plot at 0% NaCl solution exhibited the most electronegative plot configuration by reason of the deteriorating reaction of SO_4^{2-} on the steel.

1. Introduction

Stainless steel is in the group of alloys composed of a minimum of 10.5% Cr content within their metallurgical structure. The presence of Cr in addition to Mb, Ni etc. imparts exceptional mechanical and corrosion resilience characteristics as against carbon steels [1, 2]. Cr in stainless steels reacts with O_2 in aqueous industrial environments to form a passive, inert Cr_2O_3 on the steel which protects it from the action of corrosive anions [3]. Different classes and grades of stainless steels exist worldwide tailored to specific applications such as those requiring structural strength, corrosion resistance, high temperature oxidation, microbial corrosion etc. However, inappropriate selection and application of stainless steels significantly impacts their operational lifespan especially in environments that degrade stainless steels. Deterioration of stainless steel components, structures and equipment are prevalent in environments consisting of sulphate, chloride, thiosulphate ions etc. by reason of reaction of the ions with the steel's exterior. This is common in petrochemical refineries, production of fertilizers, chemical vulcanization, energy production, marine applications and desalination plants. In addition to specific of industrial operating conditions, microstructural properties, important alloy composition and ionic concentration of corrosive species significantly influences the corrosion resilience of stainless steels [4–9] making the utilization of specific steels in some environment a huge economic waste [10]. Appropriate representation of the threshold corrosion resilience of stainless steels is important for their optimal application, sustainability of industrial architecture is of utmost importance. Generally, the corrosion

resilience of stainless steels is by reason of the durability and electrochemical equilibrium of the protective oxide on their exterior [11–17]. The manuscript evaluates the threshold corrosion resistance of 434 ferritic stainless steel in 1 M H_2SO_4 electrolyte at 0.25-2% NaCl concentration. 434 stainless steel is a low carbon ferritic stainless steels with optimal corrosion resistance in mild aqueous corrosive conditions. The steel exhibits sufficient oxidation resistance at high temperatures. 434 stainless steels are ductile, not readily work hardened and can easily be fabricated.

2. Material and methods

The elemental constituents (wt. %) of 434 ferritic stainless steel (434ST) analysed with PhenomWorld scanning electron microscope as shown in Table 1. 434ST plates gotten from an automobile door trim was cut to 8 separate samples with dimensions of 1 cm^2. The 434ST were subsequently encased in vercocit resin mounts. The steels exterior was subjected to metallographic processing with SiC papers with 80, 320, 600, 800 and 1000 grits. They were subsequently burnished with 6 μm diamond burnishing fluid, and washed with purified H_2O and C_3H_6O. 200mL of 1 M H_2SO_4 was concocted in 8 different sets from analar grade H_2SO_4 solution (98%). NaCl was added to the 1 M H_2SO_4 solution at 0%, 0.25%, 0.5%, 0.75%, 1%, 1.25%, 1.5%. 1.75% and 2% NaCl concentration. Potentiodynamic polarization measurement and open circuit potential analysis was done with a tripartite wire cell system inserted within a translucent container holding 200 mL of the H_2SO_4-NaCl solution and coupled to Digi-Ivy 2311 potentiostat. Potentiodynamic polarization graphs were drawn at sweep rate of 0.0015 V/s from -0.75 V - +1.75 V. Corrosion current density, C_D (A/cm^2) and corrosion potential, C_P (V) values were gotten from Tafel extrapolation of plots sections. Corrosion rate, C_R (mm/y) was computed from the following numerical equation;

$$C_R = \frac{0.00327 \times C_D \times E_Q}{D} \tag{1}$$

E_Q illustrates equivalent weight (g) of 434ST, 0.00327 stands for corrosion rate constant and D illustrates density (g). Open circuit potential analysis of 434ST was done at step potential of 0.1V/s for 5400 s with dual-electrode cell system (Ag/AgCl standard electrode and 434ST electrode) coupled to Digi-Ivy 2311 potentiostatic instrument.

Table 1. Content (wt. %) of 434ST

434ST									
Element	P	S	C	Cr	Ni	Cu	Mn	Si	Fe
% Content	0.038	0.027	0.12	16	0.46	0.5	0.8	0.8	81.26

3. Results and discussion

3.1 Potentiodynamic polarization

The corrosion polarization graphs of 434ST in 1M H_2SO_4 at 0% to 2% NaCl concentration are illustrated in Fig. 1. Fig. 2 depicts the magnified portion of the anodic-cathodic portion of the polarization graphs. Table 2 illustrates the values gotten from the polarization test. The reaction of SO_4^{2-} and Cl^- ions in the acid electrolyte significantly influenced the electrochemical behaviour of 434ST. 434ST corrosion polarization plots exhibited anodic deviation in corrosion potential in the acid electrolyte at 0.25% to 2% Cl^- ion concentration relative to the plot from the electrolyte at 0% Cl^- ion concentration (1 M H_2SO_4 solution). At 0% Cl^- ion concentration, the corrosion potential of 434ST polarization plot is -0.462 V. However, the corrosion potential beyond this concentration varied between -0.434 V and -0.450 V. The anodic shift is by reason of the competitive reaction of SO_4^{2-} and Cl^- ions with the steel surface. The reaction of Cl^- ions in the electrolyte induces a chloride-sulphate complex on the steel surface whose effect is deleterious and at best formation of a pseudo passive oxide. Nevertheless, evolution of a passive inert oxide on the steel surface occurs through adsorption and chemical combination with dissolved O_2 in the electrolyte. The SO_4^{2-} and Cl^- ions in the electrolyte reacts with the passive oxide and engages in competitive adsorption reaction with the dissolved O_2 on the steel surface resulting to a certain degree

in chloride penetration onto the substrate Fe metal due to its smaller size. This occurrence is excercebated when there are breakages in the oxide film as a result of the possible presence of flaws within the metallurgical structure of the steel. The flaws create discontinuities that allow Cl⁻ ions and to a limited extent SO_4^{2-} to diffuse and reacts with Fe^{2+} causing its discharge into the electrolyte. The rate of discharge determines the degree of deterioration (corrosion) of 434ST. Table 2 shows the corrosion rate of 434ST in relation to Cl⁻ ion concentration. At 0% Cl⁻ ion concentration, corrosion rate of 434ST is 5.51 mm/y analogous to corrosion current density of 5.07E-04 A/cm². The corrosion rate value decreased to 1.31 mm/y at 0.25% Cl⁻ ion concentration i.e. decrease in corrosion rate of 434ST at low Cl⁻ ion concentration. However, increment in Cl⁻ ion concentration induces increase in corrosion rate of 434ST till 1% Cl⁻ ion concentration where the corrosion rate value is comparable to the value at 0% Cl⁻ ion concentration. Beyond 1% Cl⁻ concentration the corrosion rate values varied between 6.20 mm/y and 6.56 mm/y (1.25% to 2% Cl⁻ ion concentration) conveying minimal Cl⁻ ion concentration for increased deterioration of 434ST. The cathodic Tafel plot values were generally stable compared to the anodic counterparts due to stability of the H_2 evolution reactions which was less dominant compared to anodic dissolution reactions which varied significantly with respect to Cl⁻ concentration. Generally, the corrosion rate results show SO_4^{2-} ions with the presence of chlorides are deleterious to the thermodynamic stability of 434ST due to it relatively higher corrosion rate compared to 434ST at low chloride concentrations. Secondly, chloride ions have a threshold concentration were there electrochemical action has curbed effect on the corrosion resilience of 434ST. Thirdly in the presence of low chloride concentrations opposing adsorption between SO_4^{2-} and Cl⁻ ions decreases the thermodynamic inclination of 434ST to corrode.

Table 2. Potentiodynamic polarization values for 434ST corrosion in 1 M H_2SO_4 solution at 0% to 2% NaCl concentration

| Sample	NaCl Conc. (%)	Corrosion Rate (mm/y)	434ST Corrosion Current (A)	Corrosion Current Density (A/cm2)	Corrosion Potential (V)	Polarization Resistance, R_p (Ω)	Cathodic Tafel Slope, B_c (V/dec)	Anodic Tafel Slope, B_c (V/dec)
A	0	5.51	1.01E-03	5.07E-04	-0.462	25.37	-6.611	2.957
B	0.25	1.31	2.40E-04	1.20E-04	-0.450	68.69	-7.264	2.246
C	0.5	3.10	5.71E-04	2.85E-04	-0.434	45.03	-7.888	4.306
D	0.75	3.84	7.07E-04	3.53E-04	-0.436	40.37	-8.082	6.468
E	1	5.97	1.10E-03	5.49E-04	-0.448	22.37	-7.111	5.519
F	1.25	6.56	1.21E-03	6.03E-04	-0.446	16.30	-7.327	6.468
G	1.5	6.20	1.14E-03	5.70E-04	-0.439	18.53	-8.200	5.109
H	1.75	6.25	1.15E-03	5.75E-04	-0.442	18.48	-7.781	6.351
I	2	6.36	1.17E-03	5.85E-04	-0.443	19.49	-8.609	7.615
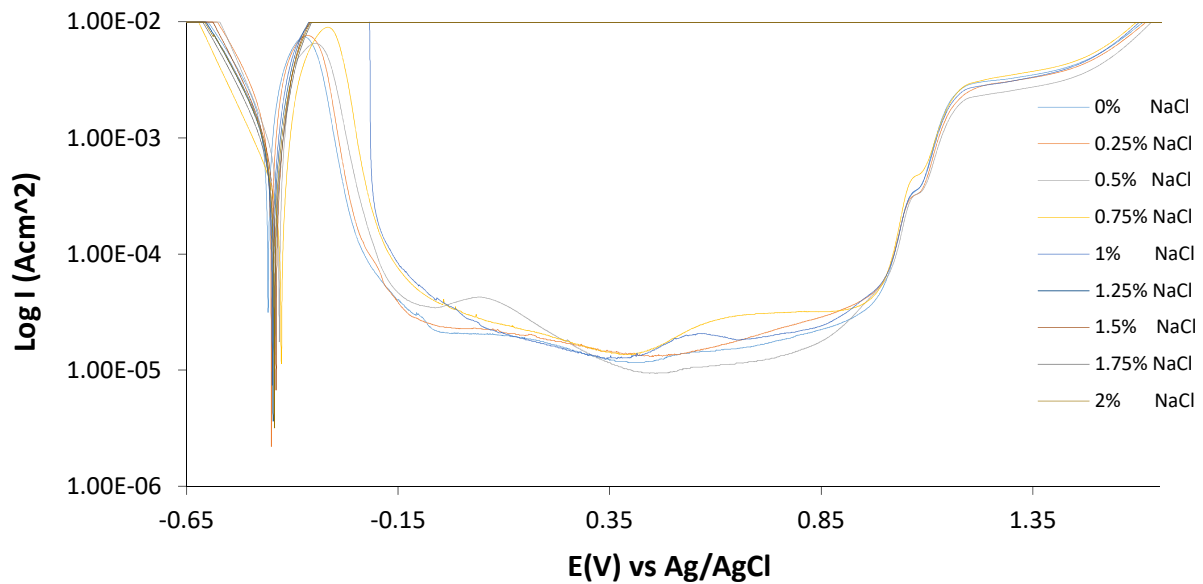
Figure. 1. Potentiodynamic polarization graphs for 434ST corrosion in 1 M H_2SO_4 solution at 0% to 2% NaCl concentration
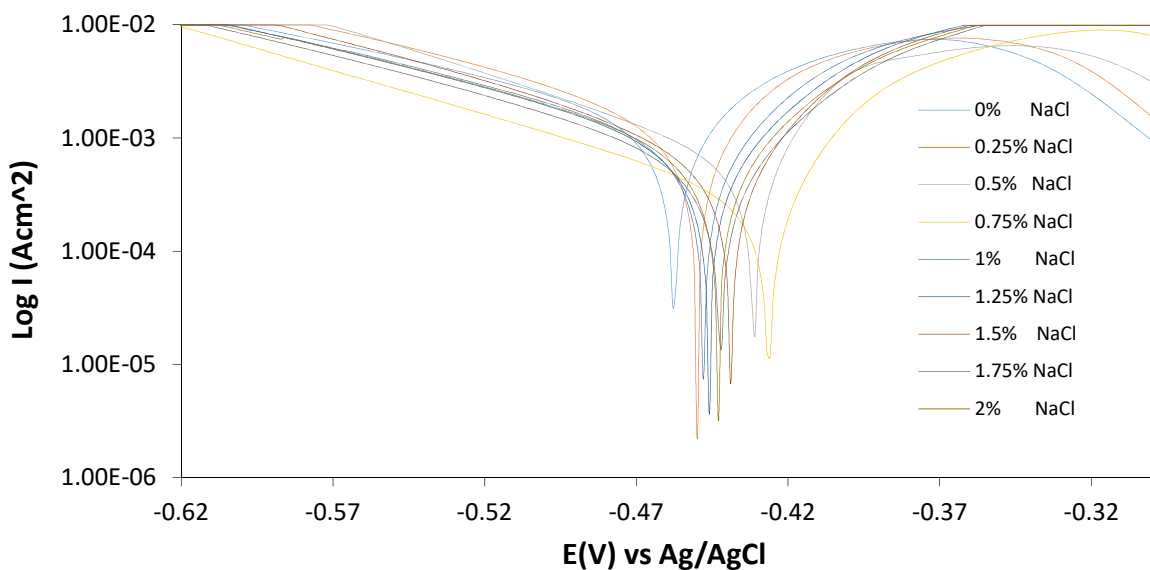

Figure. 2. Magnified view of the anodic-cathodic polarization plots for 434ST corrosion in 1 M H_2SO_4 solution at 0% to 2% NaCl concentration

3.2 Open circuit potential analysis

Open circuit potential graphs for 434ST in 1 M H_2SO_4 at 0%, 0.25% and 2% Cl^- ion concentration are illustrated in Fig. 3. Generally, the potential plots at 2% Cl^- ion concentration exhibited the most electropositive potential displacement while the plots at 0% Cl^- ion concentration exhibited the most electronegative displacement. The plot at 2% Cl^- ion concentration started at -0.442 V (0 s) and steeply deviated to electronegative potentials till -0.457 V at 300 s due to initial surface oxidation of the steel resulting from the synergistic reaction effect of SO_4^{2-} and Cl^- ions inside the electrolyte. This occurs when the protective inert oxide on the steel is yet to completely offer meaningful protection. Beyond 300 s of exposure the potential of the steel progressively shifts to electropositive potential as the

protective oxide achieves relative stability and continues to grow. The potential plot at 0% Cl^- ion concentration at -0.460 V (0 s) and shifted to -0.466 V at 107.70 s by reason of anodic reaction of the steel exterior in the vicinity of SO_4^{2-} ions. However, the electronegative portion of the potential plot is significantly shorter than the one observed for the plot at 2% Cl^- ion concentration. This is by reason of the relatively large size of SO_4^{2-} ions compared to Cl^- ions which can more easily diffuse through the protective film on the steel. As a result, evolution of the oxide occurred at much shorter time. Beyond -0.466 V, electropositive shift of the plots was visible till -0.448 V at 5400 s. The final plot configuration at 2% and 0% Cl^- ion concentration shows the presence of Cl^- ions with SO_4^{2-} though debilitating increases the corrosion resistance of 434ST compared to SO_4^{2-} ions only. The potential plot at 0.25% Cl- ion concentration displayed near similar plot configuration with the plot at 0% Cl^- ion concentration, though its electronegative potential portion of the plot is visibly shorter and the final potential at 5400 s is more electropositive at -0.446 V.
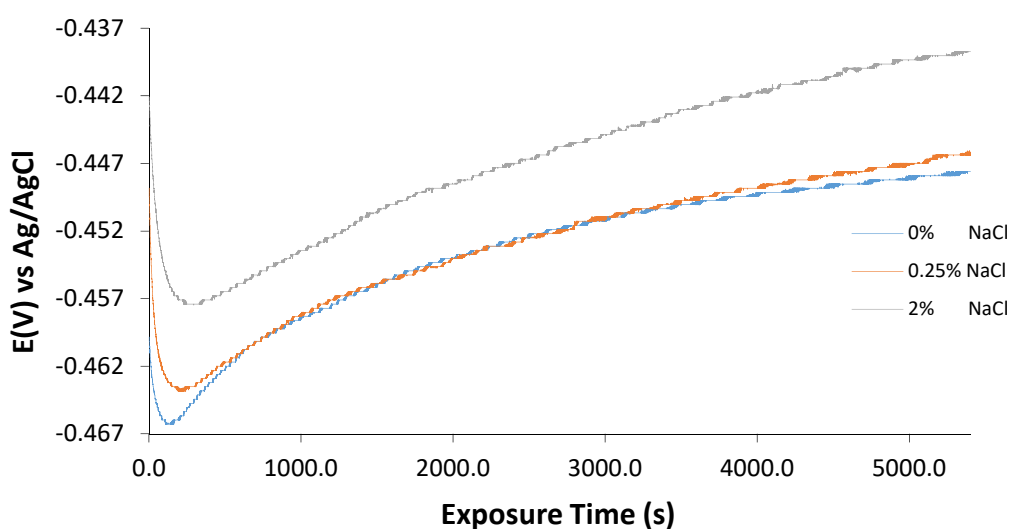

Figure. 3. Open circuit potential graphs of 434ST corrosion in 1 M H_2SO_4 solution at 0%, 0.25% and 2% Cl^- ion concentration

4. Conclusion

434 ferritic stainless steel exhibited limited resistance to corrosion in the presence of SO_4^{2-} ions. In the face of low concentrations of Cl^- ions, corrosion of 434 steel decreased significantly due to competitive adsorption and reaction processes with the steel. Increment in Cl^- ion concentration caused progressive increase in corrosion rate till a threshold chloride value were the corrosion rate was relatively high compared to the solution in absence of Cl^- ions. Polarization plots showed significant anodic shift by reason of evolution of protective inert oxide on the steel. Open circuit potential plots depict the presence of Cl^- ions increases the passive protective on the steel hence its corrosion resilience compared to the plot in the absence of chlorides.

Acknowledgement

References

[1] Black, J. (2006). Biological performance of materials: Fundamentals of Biocompatibility. 4th ed. Boca Raton: CRC Press.

[2] Číhal, V. (1999). Stainless steels and alloys. (in Czech). Praha: Academia.

[3] Incoloy Alloy 800H & 800HT, Technical Bulletin, Special Metals Publication SMC- 047. http://www.specialmetals.com [Retrieved 1st April, 2019].

[4] Liptáková, T. (2011). Pitting corrosion of stainless steels. Materials Engineering, 18, 115–20.

[5] Szklarska Salowska, Z. (2005). Pitting and crevice corrosion. Houston Texas: NACE International.

[6] Rodabaugh, R.D. (1999). Surface cleaning. ASM Handbook. 3rd ed. USA: ASM International.

[7] Feng, H., Li, H., Wu, X., Jiang, Z., Zhao, Si., & Zhang T, et al. (2018). Effect of nitrogen on corrosion behaviour of a novel high nitrogen medium-entropy alloy CrCoNiN manufactured by pressurized metallurgy, Journal of Materials Science and Technology, 34(10), 1781–1790.

[8] Burstein, G.T., & Pistorious, P.C. (1995). Surface roughness and the metastable pitting of stainless steel in chloride solutions, Corrosion, 51(5), 380–385.

[9] Zhang, S., Li, H., Jiang, Z., Zhang, B., Li, Z., & Wu, J. et al. (2019). Effects of Cr and Mo on precipitation behavior and associated intergranular corrosion susceptibility of superaustenitic stainless steel S32654, Materials Characterization, 152, 141–150.

[10] Burkert, A., Lehmann, J., Burkert, A., Mietz, J., & Gumpel, P. (2013). Technical and economical stainless steel alternatives for civil engineering applications, Materials and Corrosion, 64, 1–17.

[11] Lee, J.B. (2006). Effects of alloying elements, Cr, Mo and N on repassivation characteristics of stainless steels using the abrading electrode technique, Materials Chemistry and Physics, 99(2–3), 224–234.

[12] Loto, R.T., & Loto, C.A. (2019). Evaluation of the localized corrosion resistance of 316 L austenitic and 430Ti ferritic stainless steel in aqueous chloride/sulphate media for application in petrochemical crude distillation units, Materials Research Express, 6, 086516. https://doi.org/10.1088/2053-1591/ab1a11.

[13] Loto, R.T. (2018). Potentiodynamic polarization studies of the pitting corrosion resistance and passivation behavior of P4 low carbon mold steel in chloride and acid chloride solution, Material Research Express, 5, 116509https://doi.org/10.1088/2053-1591/ aadc84.

[14] Loto, R.T. (2018). Effect of elevated temperature on the corrosion polarization of NO7718 and NO7208 nickel alloys in hot acid chloride solution, Journal of Bio and Tribo Corrosion, 4(71). https://doi.org/10.1007/s40735-018-0190-8.

[15] Loto, R.T., & Loto, C.A. (2017). Potentiodynamic polarization behavior and pitting corrosion analysis of 2101 duplex and 301 austenitic stainless steel in sulfuric acid concentrations, Journal of Failure Analysis and Prevention, 17(4), 672–679. https://doi.org/10.1007/s11668- 017-0291-6.

[16] Loto, R.T. (2017). Study of the corrosion resistance of type 304L and 316 austenitic stainless steels in acid chloride solution, Oriental Journal of Chemistry, 33(3), 1090–1096. https://doi.org/ 10.13005/ojc/330304.

[17] Loto, R.T. (2017). Electrochemical corrosion characteristics of 439 ferritic, 301 austenitic, S32101 duplex and 420 martensitic stainless steel in sulfuric acid/NaCl solution, Journal of Bio and Tribo Corrosion, 3(24). https://doi.org/10.1007/s40735-017-0084-1